

# The $Z \rightarrow \tau\tau \rightarrow (\tau_{jet}\nu_\tau)(l\nu_l\nu_\tau)$ analysis with ATLAS detector with early data

**Daniele Capriotti**

Max Planck Institut fuer Physik  
Werner Heisenberg Institut  
Muenchen, 80805, Germany  
capriott@mppmu.mpg.de

Young Scientists Workshop @ Ringberg Casle



# Overview

- Introduction
- Tau reconstruction and identification with the ATLAS detector
- The  $Z \rightarrow \tau\tau$  analysis with early data
- Conclusion

# Introduction

## Why W/Z Boson physics?

- The study of the W and Z Boson production and their properties will be one of the most important measurements of ATLAS during the first phase of LHC.
- By measuring the inclusive production cross-section, we are able to test theoretical QCD predictions at an unknown energy regime.
- The measurement of the differential production cross-sections, e.g. vs. rapidity, transverse momentum and charge, will give new constraints on the structure functions of the proton.
- Knowing these to a high precision is absolutely necessary to conduct electroweak precision measurements, such as the W-mass measurement, at a later stage of the experiment.
- Understanding the W and Z boson production and their properties is a major ingredient for most of the searches for physics beyond the Standard Model.

## Why $\tau$ lepton final state?

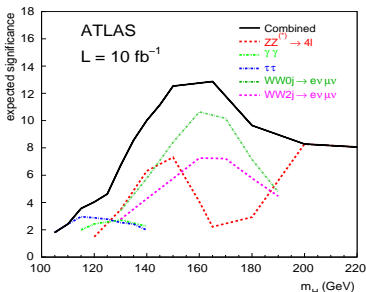
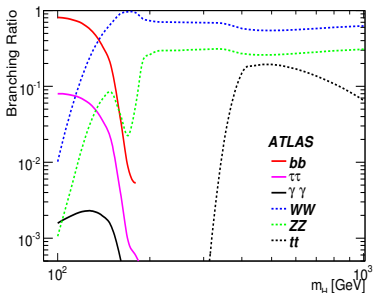
Tau reconstruction is an important (and challenging!) task:

Understanding of the detector:

- Measurement of the  $\tau$  energy scale
- Measurement of the  $E_T^{miss}$  scale

Physics motivations:

- Measurement of W/Z production cross section
- Discovery of the SM and MSSM Higgs boson in  $\tau\tau$  final state



# Basic Tau Properties

## TAU BRANCHING RATIOS

Leptonic Modes (35%)

$e\nu_e\nu_\tau$  18%

$\mu\nu_\mu\nu_\tau$  17%

Hadronic Modes: 1 Prong (47%)

$\pi^-\nu_\tau$  11%

$\pi^-\pi^0\nu_\tau$  25%

$\pi^-\pi^0\pi^0\nu_\tau$  9%

$\pi^-\pi^0\pi^0\pi^0\nu_\tau$  1%

$K^- + \text{Neutrals}$  1.5%

Hadronic Modes: 3 Prong (15%)

$\pi^-\pi^+\pi^-\nu_\tau$  9%

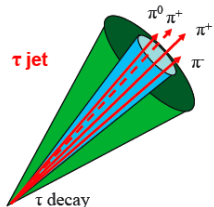
$\pi^-\pi^+\pi^-\pi^0\nu_\tau$  4.5%

$K^-\pi^+\pi^-\nu_\tau$  0.4%

Other Modes ( $\approx 3\%$ )

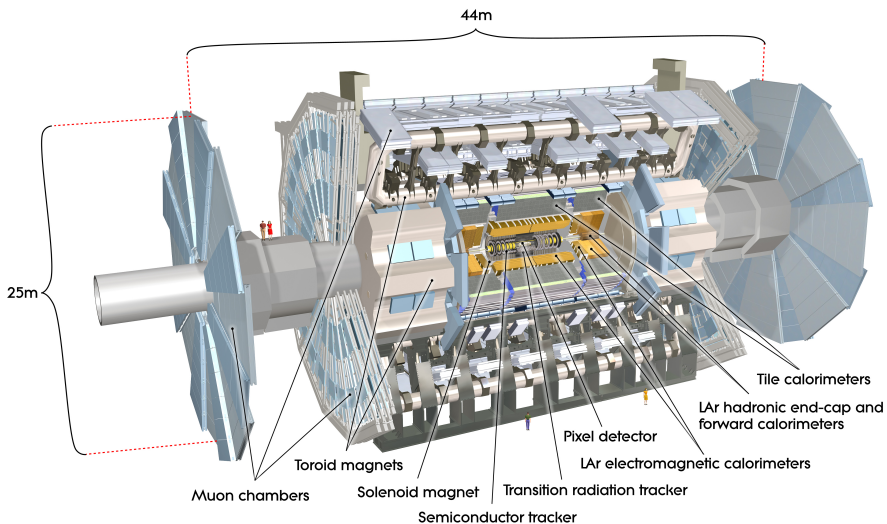
## TAU CHARACTERISTICS

- $m_\tau \approx 1.8$  GeV
- $c\tau = 87$   $\mu\text{m}$
- Hadronic decays are well collimated collection of charged and neutral pions/kaons: leading particle direction reproduces  $\tau$  direction well
- 1 or 3 charged tracks in the  $\tau$ -jet



# Tau reconstruction and identification with the ATLAS detector

# The ATLAS detector at LHC





# Tau reconstruction in ATLAS

⇒ The  $\tau$  reconstruction and ID refer to hadronically decaying  $\tau$  leptons.

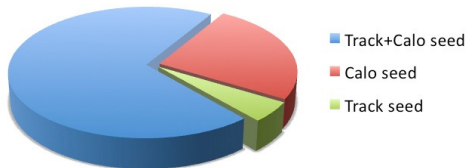
## Track seed algorithm

- ➊ Seed track with  $p_T > 6 \text{ GeV}$  with good quality criteria.
- ➋ Association with other tracks in  $\Delta R < 0.2$  with quality criteria.
- ➌ Total charge  $|Q| = 1$ .
- ➍ Energy flow algorithm

## Calorimeter seed algorithm

- ➊ Jets with  $E_T > 10 \text{ GeV}$ .
- ➋ Tracks associated if  $\Delta R < 0.3$ , passing minimal quality criteria.
- ➌ Energy calculation summing the weighted calorimeter cells in  $\Delta R < 0.4$

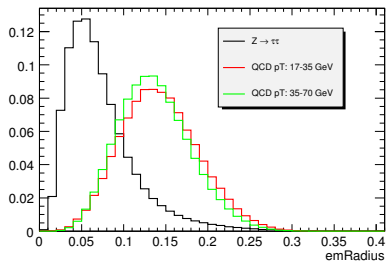
**Calorimeter + Track seeds** matched if  $\Delta R < 0.2$



# Tau Identification with early data: Safe Identification

- "Safe-variables": discriminating variables for the  $\tau$ -ID in the early data ("Safe"  $\Rightarrow$  small sensitivity to detector-related systematic uncertainties).
- Not used with early data: variables based on: precision tracking,  $\pi^0$  reconstruction ...

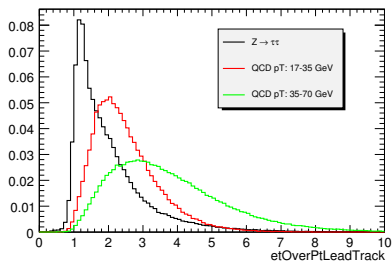
Electromagnetic Radius  $R_{em}$



$$R_{em} = \frac{\sum_{i=1}^{\Delta R < 0.4} E_{T,i} \sqrt{(\eta_i - \eta)^2 + (\phi_i - \phi)^2}}{\sum_{i=1}^{\Delta R < 0.4} E_{T,i}}$$

$i$  calorimetric cell,  $E_T$   $\eta_i$   $\phi_i$  measured in the EM calorimeter,  $\eta$   $\phi$  seeded tau coordinates.

Ratio  $E_T/p_T$  of the leading track

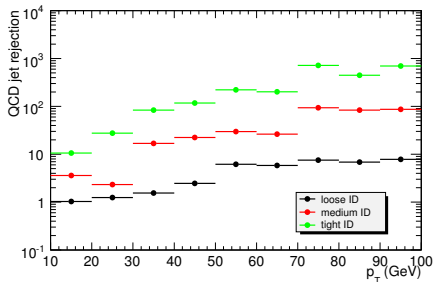
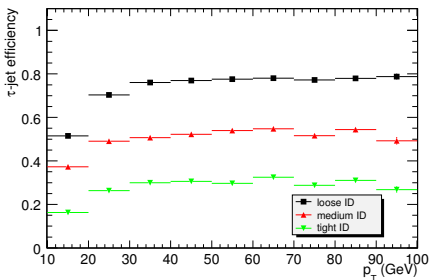


$$E_T^{total}/p_{T1} = \frac{\sum_{i=1} E_{T,i}^{EM} + \sum_{i=1} E_{T,i}^{Had}}{p_{T1}}$$

$i$  calorimetric cell,  $p_{T1}$  momentum of the leading track

# Taujet efficiency and QCD jet rejection

"Safe Cut" with Calorimeter+Track seed



- *Tight, medium, loose* cuts corresponding to 0.3, 0.5, 0.7  $\tau$ -jet efficiency
- Identification criteria optimized separately for 5  $p_T$  bins (10-25 GeV, 25-45 GeV, 45-70 GeV, 70-100 GeV, > 100 GeV) separately for 1-prong or 3-prong candidates.

# Electron Reconstruction

Different reconstruction algorithms: Calo seed or Track seed

- **Calo Seed**: starts from clusters reconstructed in the calorimeters and then builds the identification variables based on info from the inner detector and EM calorimeters
- **Track Seed**: selects good-quality tracks matching a relatively isolated deposition of energy in the EM calorimeters. The identification variables are then calculated in the same way as for the Calo Seed algorithm

The standard identification of high- $p_T$  electrons is based on many cuts which can all be applied independently. These cuts have been optimized in up to seven bins in  $\eta$  and six bins in  $p_T$ .

Definition of 3 different cuts:

- **Loose** simple electron identification based only on limited calorimetric info. Cuts applied on the hadronic leakage and on shower-shape variables, derived from the middle layer of the EM calo
- **Medium** same as loose but adding cuts on the strips in the first layer of EM calo and on the tracking variables
- **Tight** use of particle identification tool. Cutting on more variables than the Medium case.

## Muon Reconstruction

Different strategies, corresponding to different ways to combine data from more ATLAS subdetectors:

- **standalone reconstruction algorithms:** tracks from the Muon Spectrometer backtracked to the interaction point
- **combined reconstruction algorithms:** tracks from the Inner Detector combined with full Muon Spectrometer tracks
- **segment tagging algorithms:** tracks from the Inner Detector extrapolated to the Muon Spectrometer and combined with segments reconstructed in Muon Spectrometer stations
- **calorimeter tagging algorithms:** tracks from the Inner Detector with a MIP energy deposit in the Calorimeters.

## The $Z \rightarrow \tau\tau$ selection

$Z \rightarrow \tau\tau$  in early data

Goal: reconstruct a clean sample of  $Z \rightarrow \tau\tau$  events. This allows for:

- understanding of the  $\tau$ -jet reconstruction
- understanding of the background in SM and MSSM Higgs search

Presented analysis performed in order to deal with early data ( $100 \text{ pb}^{-1}$ ) at 10 TeV.

	$\sigma \text{ (nb)}$	$\epsilon_{filter}$	Nr. events for $100 \text{ pb}^{-1}$
$Z \rightarrow \tau^+\tau^-$	<b>1.128 (LO)</b>	<b>1</b>	<b>112800</b>
$Z \rightarrow e^+e^-$	1.144 (LO)	0.96	109824
$Z \rightarrow \mu^+\mu^-$	1.144 (LO)	0.96	109824
$W \rightarrow e\nu_e$	11.765 (LO)	0.88	1035320
$W \rightarrow \mu\nu_\mu$	11.765 (LO)	0.88	1035320
$W \rightarrow \tau_{lep}\nu_\mu$	4.148 (LO)	0.87	360876
$W \rightarrow \tau_{had}\nu_\mu$	7.690 (LO)	1	769000
$t\bar{t}$	0.374 (NLO)	0.55	20570
QCD dijet (1e filter) $p_T$ 17-35 GeV	$8.668 \cdot 10^5$	$1.09 \cdot 10^{-3}$	$94.5 \cdot 10^6$
QCD dijet (1e filter) $p_T$ 35-70 GeV	$5.601 \cdot 10^4$	$5.45 \cdot 10^{-3}$	$30.5 \cdot 10^6$
QCD dijet (1 $\mu$ filter) $p_T$ 17-35 GeV	$8.668 \cdot 10^5$	$1.02 \cdot 10^{-3}$	$88.4 \cdot 10^6$
QCD dijet (1 $\mu$ filter) $p_T$ 35-70 GeV	$5.601 \cdot 10^4$	$5.11 \cdot 10^{-3}$	$28.6 \cdot 10^6$

- samples analysed with full detector simulation
- factorization of QCD background

# Selection of the $Z \rightarrow \tau\tau \rightarrow (\tau_{jet}\nu_\tau)(l\nu_l\nu_\tau)$ signature

## Medium Electrons

- $p_T > 15 \text{ GeV}$ ,  $|\eta| < 2.5$  and  $|Q| = 1$
- Identification flag: medium
- Isolation:  $E_T$  (in cone  $\Delta R < 0.40$ ) /  $p_T < 0.12$ .

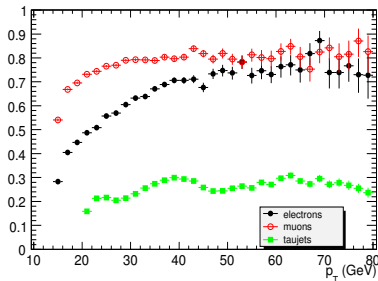
## Combined muons

- $p_T > 15 \text{ GeV}$ ,  $|\eta| < 2.5$  and  $|Q| = 1$
- Identification: combined (inner tracker + muon spectrometer)
- Isolation:  $E_T$  (in cone  $\Delta R < 0.40$ ) /  $p_T < 0.10$  and no tracks in cone 0.40.

## TauJets

- $E_T > 20 \text{ GeV}$ ,  $|\eta| < 2.5$  and  $|Q| = 1$
- Tau identification with tight safe variables
- Remove overlap between taujets and combined muons (and medium electron) in  $\Delta R < 0.30$
- Electron veto

- Efficiency after selection criteria on the left





# Signal Selection

⇒ Combining 1 taujet and 1 lepton (e,μ) with opposite charge  
 ("OppositeSign")

⇒ Suppression of  $W \rightarrow e(\mu)\nu$  background:

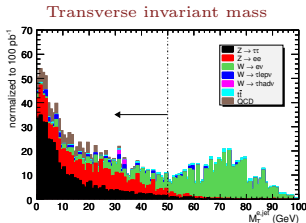
- cut on the transverse invariant mass

$$m_T^{lep,miss} = \sqrt{2p_T^{lep} E_T^{miss} (1 - \cos \phi_{lep,miss})}$$

- cut on the collinearity between lepton and missing energy
- cut on the  $\Delta R$  between lepton and  $\tau$ -jet

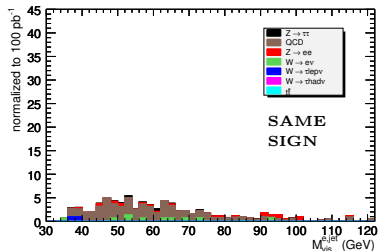
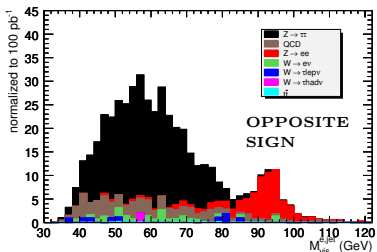
⇒ Counting events in the visible invariant mass windows ( $M_{vis}$ , invariant mass of lepton and  $\tau$ -jet)

⇒ Background control with same-sign ( $\tau$ , lepton) selection ("SameSign").



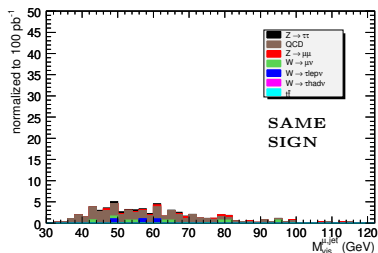
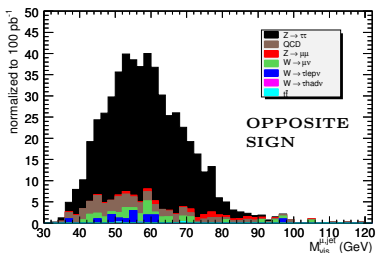
# Results for the $Z \rightarrow \tau\tau \rightarrow (\tau_{jet}\nu_\tau)(e\nu_e\nu_\tau)$ analysis

	$Z \rightarrow \tau^+\tau^-$	$Z \rightarrow e^+e^-$	$W \rightarrow e\nu$	$W \rightarrow \tau\nu$	$W \rightarrow \tau_h\nu$	$t\bar{t}$	QCD
Presel $1e+1\tau_{jet}$	<b>450±7</b>	416±11	772 ±22	52 ±7	6 ±3	91 ±2	235±46
Opposite Sign							
$1e+1\tau_{jet}$	<b>442±7</b>	354±10	580±19	37±6	4±3	79±2	120±33
$m_T^{e,miss} < 50 \text{ GeV}$	<b>431±7</b>	337±10	141±10	31±5	4±3	24±1	120±33
angular correl > -0.15	<b>408±7</b>	248±8	50±6	17±4	2±2	19±1	86±22
$2.1 < \Delta R < 4.1$	<b>368±7</b>	232±8	43±6	14±4	2±2	9±1	73±19
$p_T^{ele} < 35 \text{ GeV}$	<b>330±6</b>	71±4	20±4	9±3	2±2	3.0±0.4	71±19
$p_T^{\tau_{jet}} < 60 \text{ GeV}$	<b>326±6</b>	65±4	18±3	8±3	2±2	2.7±0.3	69±19
$35 < M_{vis} < 80 \text{ GeV}$	<b>317±6</b>	11±2	16±3	6±2	2±2	1.7±0.3	60±18
Same Sign							
$1e+1\tau_{jet}$	<b>7±1</b>	62±4	192±11	15±4	2±2	12±1	115±32
$m_T^{e,miss} < 50 \text{ GeV}$	<b>7±1</b>	57±4	35±5	8±3	2±2	4.0±0.4	114±32
angular correl > -0.15	<b>5±1</b>	41±3	18±3	3±2	<1.6	3.3±0.4	84±23
$2.1 < \Delta R < 4.1$	<b>4±1</b>	30±3	12±3	2±1	<1.6	1.7±0.4	66±17
$p_T^{ele} < 35 \text{ GeV}$	<b>3±1</b>	8±1	7±2	2±1	<1.6	0.3±0.1	64±17
$p_T^{\tau_{jet}} < 60 \text{ GeV}$	<b>3±1</b>	8±1	7±2	2±1	<1.6	0.3±0.1	62±17
$35 < M_{vis} < 80 \text{ GeV}$	<b>2±1</b>	4±1	5±2	2±1	<1.6	0.2±0.1	55±16



# Results for the $Z \rightarrow \tau\tau \rightarrow (\tau_{jet}\nu_\tau)(\mu\nu_\mu\nu_\tau)$ analysis

	$Z \rightarrow \tau^+\tau^-$	$Z \rightarrow \mu^+\mu^-$	$W \rightarrow \mu\nu$	$W \rightarrow \tau\nu$	$W \rightarrow \tau_h\nu$	$t\bar{t}$	QCD
Presel $1\mu+1\tau_{jet}$	<b>600±8</b>	143±6	906±24	62±8	<1.6	97±2	179±37
OppositeSign							
$1\mu+1\tau_{jet}$	<b>590±8</b>	102±5	689±21	47±7	<1.6	84±2	95±28
$m_T^{\mu,miss} < 50 \text{ GeV}$	<b>573±8</b>	74±4	157±10	36±6	<1.6	24±1	95±28
angular correl > -0.15	<b>537±8</b>	49±3	55±6	18±4	<1.6	19±1	67±19
$2.1 < \Delta R < 4.1$	<b>489±8</b>	43±3	46±6	17±4	<1.6	9±1	55±16
$p_T^{ele} < 35 \text{ GeV}$	<b>444±7</b>	14±2	26±4	15±4	<1.6	3.4±0.4	54±16
$p_T^{\tau_{jet}} < 60 \text{ GeV}$	<b>440±7</b>	13±2	25±4	13±3	<1.6	2.8±0.3	53±16
$35 < M_{vis} < 80 \text{ GeV}$	<b>430±7</b>	10±1	22±4	12±3	<1.6	2.0±0.3	48±15
SameSign							
$1\mu+1\tau_{jet}$	<b>10±1</b>	41±3	216±12	15±4	<1.6	12±1	84±24
$m_T^{\mu,miss} < 50 \text{ GeV}$	<b>10±1</b>	27±2	49±6	9±3	<1.6	4.6±0.4	84±24
angular correl > -0.15	<b>7±1</b>	17±2	22±4	5±2	<1.6	3.4±0.4	59±17
$2.1 < \Delta R < 4.1$	<b>6±1</b>	13±2	18±4	3±2	<1.6	1.8±0.4	48±14
$p_T^{ele} < 35 \text{ GeV}$	<b>5±1</b>	4±1	7±2	3±2	<1.6	0.4±0.1	48±14
$p_T^{\tau_{jet}} < 60 \text{ GeV}$	<b>4±1</b>	4±1	6±2	3±2	<1.6	0.3±0.1	47±13
$35 < M_{vis} < 80 \text{ GeV}$	<b>4±1</b>	3±1	5±2	3±2	<1.6	0.3±0.1	42±13



# Conclusion

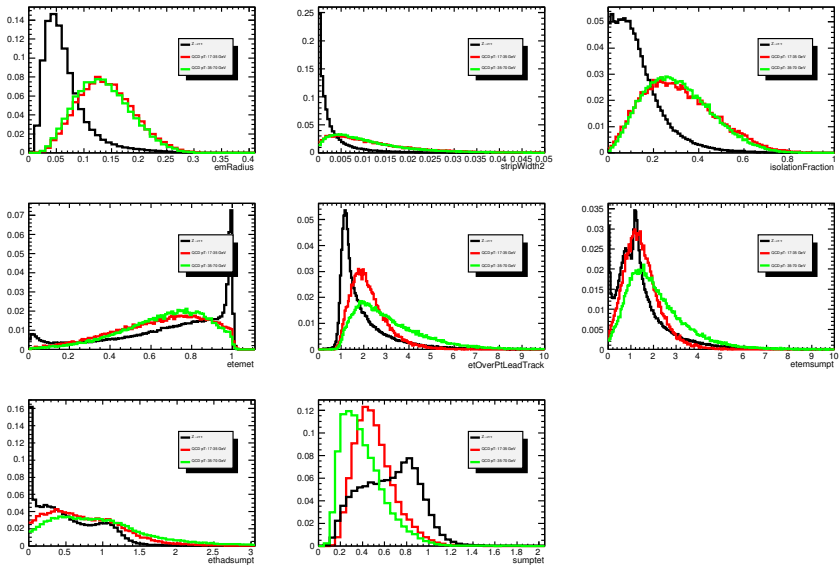
- Up to now less than  $200 \text{ nb}^{-1}$  of data  $\Rightarrow$  no signal event passes the selection.
- $Z \rightarrow \tau\tau$  analysis optimized for early data ( $100 \text{ pb}^{-1}$ ): good identification of the  $\tau$ -jets and separation from the QCD background.
- Data driven estimation of the QCD background from the Same Sign control data sample
- Extend the analysis to the  $Z + \text{jet}$  final state (dominant background for SM Higgs searches in the  $\tau\tau$  final state)



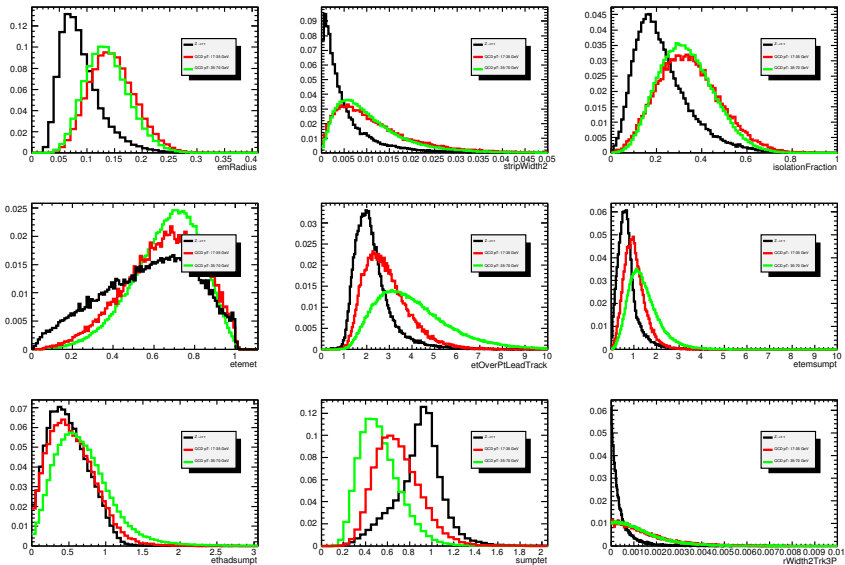
## Backup Slides

- Safe variables for tau identification
- Factorization of the QCD background
- Transverse mass with missing energy and angular correlation
- Results with loose lepton isolation

## Safe variables for 1 prong taujets



# Safe variables for 3 prong taujets





## Factorization of the QCD background

Due to low MC statistics for QCD background, its contribution has to be estimated from factorization procedure.

**Procedure:**

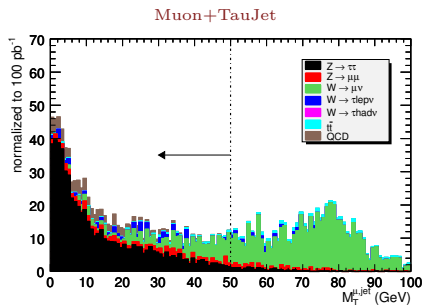
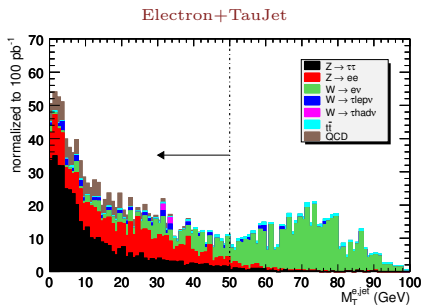
- ① Performing the analysis with no safe ID cuts on  $\tau$ -jets and avoiding lepton isolation (cut on  $E_T/p_T$  and number of tracks in cone)
- ② Efficiencies of the lepton isolation and  $\tau$ -jet identification are calculated separately: no correlation found with the other cuts applied in the analysis
- ③ QCD events weighted by the efficiency of the lepton isolation and  $\tau$ -jet identification

lepton isolation efficiency	QCD pT: 17-35 GeV, 1 electron filter 0.0359 $\pm$ 0.0110	QCD pT: 35-70 GeV, 1 electron filter 0.0224 $\pm$ 0.0032
$\tau$ -jet identification efficiency	0.0229 $\pm$ 0.0087	0.0149 $\pm$ 0.0026
lepton isolation efficiency	QCD pT: 17-35 GeV, 1 muon filter 0.0158 $\pm$ 0.0048	QCD pT: 35-70 GeV, 1 muon filter 0.0024 $\pm$ 0.0005
$\tau$ -jet identification efficiency	0.0274 $\pm$ 0.0063	0.0140 $\pm$ 0.0012

# Transverse invariant mass

- Transverse invariant mass lepton + missing energy:

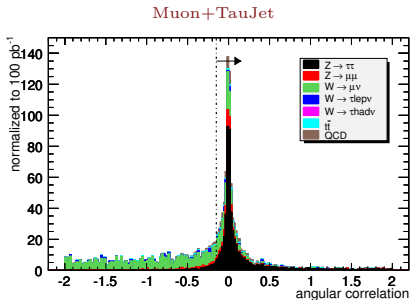
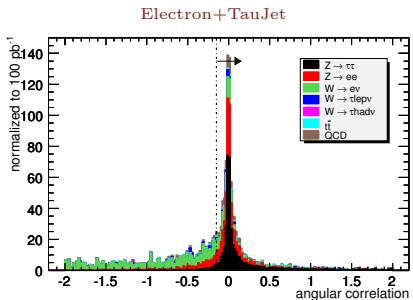
$$m_T = \sqrt{2p_T^{lep} E_T^{miss} (1 - \cos \phi_{lep,miss})}$$



- $m_T^{lep,miss} < 50$  GeV for the analysis

# Angular Correlation

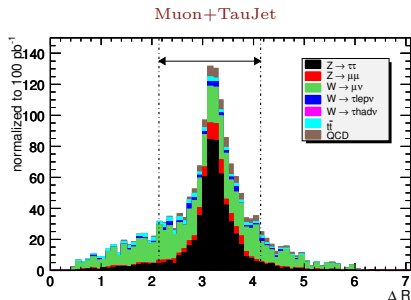
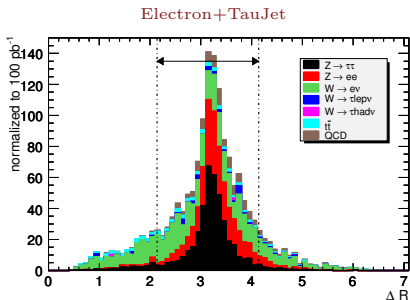
- Angular Correlation:  $\Delta\psi = \cos(\phi_{lep} - \phi_{miss}) + \cos(\phi_{jet} - \phi_{miss})$



- $\Delta\psi > -0.15$

## Distance between lepton- $\tau_{jet}$

- Distance between the two visible particles:  $\Delta R = \sqrt{\Delta\phi^2 + \Delta\theta^2}$



- $2.14 < \Delta R_{lep,\tau_{jet}} < 4.14$  for the analysis

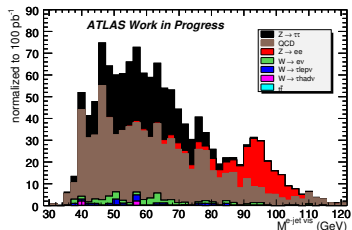
# Old results for the $Z \rightarrow \tau\tau \rightarrow e\tau_{jet}$ analysis

Looser lepton isolation in order to compare SS and OS events with higher statistics

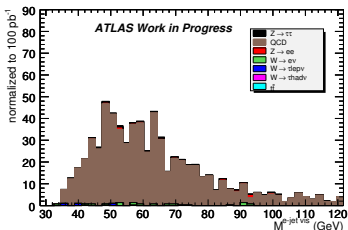
Number of events shown after trigger selection [trigger efficiency in brackets]

	$Z \rightarrow \tau^+\tau^-$	$Z \rightarrow e^+e^-$	$W \rightarrow e\nu$	$W \rightarrow \tau\nu$	$W \rightarrow \tau_h\nu$	$t\bar{t}$	QCD
Presel $1e+1\tau_{jet}$	<b>508±8</b>	746±14	764 ±22	60 ±7	6 ±3	80 ±2	1759 ± 256
Opposite Sign (OS)							
$1e+1\tau_{jet}$	<b>497±7</b>	668±14	567±19	47±7	4±3	69±2	908 ± 134
$m_T^{e,miss} < 35 \text{ GeV}$	<b>457±7</b>	511±12	78±7	31±5	4±3	14±1	885 ± 130
$2.1 < \Delta R < 4.1$	<b>415±7</b>	464±11	61±6	23±5	4±3	6.6±0.5	714 ± 105
$p_T^{e\tau} < 35 \text{ GeV}$	<b>385±7</b>	182±7	49±6	19±4	4±3	2.9±0.3	700 ± 103
$p_T^{\tau_{jet}} < 60 \text{ GeV}$	<b>380±6</b>	161±7	45±5	17±4	4±3	2.4±0.3	667 ± 97
$35 < M_{vis} < 80 \text{ GeV}$	<b>369±6 [0.97]</b>	24±3 [1]	38±5 [1]	15±4 [1]	4±3 [1]	1.5±0.3 [1]	550 ± 80 [0.99]
Same Sign (SS)							
$1e+1\tau_{jet}$	<b>10±1</b>	78±5	197±11	13±3	2±2	11±1	850 ± 126
$m_T^{e,miss} < 35 \text{ GeV}$	<b>9±1</b>	61±4 [	18±3	6±2	<1.6	2.8±0.3	831 ± 123
$2.1 < \Delta R < 4.1$	<b>7±1</b>	44±3	13±3	3±2	<1.6	1.3±0.2	654 ± 98
$p_T^{e\tau} < 35 \text{ GeV}$	<b>7±1</b>	16±2	10±3	3±2	<1.6	0.4±0.1	639 ± 96
$p_T^{\tau_{jet}} < 60 \text{ GeV}$	<b>6±1</b>	15±2	10±3	3±2	<1.6	0.4±0.1	610 ± 91
$35 < M_{vis} < 80 \text{ GeV}$	<b>6±1 [1]</b>	7±1 [1]	7±2 [1]	3±2 [1]	<1.6	0.3±0.1 [1]	505 ± 75 [0.99]

Electron+TauJet Opposite Sign



Electron+TauJet Same Sign



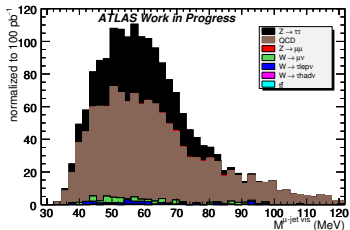
# Old results for the $Z \rightarrow \tau\tau \rightarrow \mu\tau_{jet}$ analysis

Looser lepton isolation in order to compare SS and OS events with higher statistics

Number of events shown after trigger selection [trigger efficiency in brackets]

	$Z \rightarrow \tau^+\tau^-$	$Z \rightarrow \mu^+\mu^-$	$W \rightarrow \mu\nu$	$W \rightarrow \tau\nu$	$W \rightarrow \tau h\nu$	$t\bar{t}$	QCD
Presel $1\mu+1\tau_{jet}$	<b>613±8</b>	134±5	901±24	57±7	<1.6	106±2	2685 ± 407
Opposite Sign (OS)							
$1\mu+1\tau_{jet}$	<b>602±8</b>	96±5	674±21	44±6	<1.6	91±2	1373 ± 208
$m_T^{\mu,miss} < 35 \text{ GeV}$	<b>540±8</b>	52±3	66±7	29±5	<1.6	17±1	1317 ± 199
$2.1 < \Delta R < 4.1$	<b>492±7</b>	47±3	53±6	24±5	<1.6	9±1	1062 ± 162
$p_T^{le} < 35 \text{ GeV}$	<b>457±7</b>	18±2	40±5	21±4	<1.6	4.2±0.4	1049 ± 159
$p_T^{\tau_{jet}} < 60 \text{ GeV}$	<b>452±7</b>	17±2	37±5	20±4	<1.6	3.3±0.4	972 ± 146
<b><math>35 &lt; M_{vis} &lt; 80 \text{ GeV}</math></b>	<b>440±7 [0.86]</b>	13±2 [0.93]	30±4 [0.97]	18±4 [0.95]	<1.6	2.2±0.3 [1]	771 ± 114 [0.80]
Same Sign (SS)							
$1\mu+1\tau_{jet}$	<b>11±1</b>	38±3	226±12	13±3	<1.6	14±1	1312 ± 201
$m_T^{\mu,miss} < 35 \text{ GeV}$	<b>9±1</b>	16±2	22±4	4±2	<1.6	2.6±0.3	1254 ± 191
$2.1 < \Delta R < 4.1$	<b>7±1</b>	10±1	17±3	2±1	<1.6	1.3±0.2	1014 ± 156
$p_T^{le} < 35 \text{ GeV}$	<b>6±1</b>	5±1	12±3	2±1	<1.6	0.5±0.1	1000 ± 153
$p_T^{\tau_{jet}} < 60 \text{ GeV}$	<b>5±1</b>	5±1	11±3	2±1	<1.6	0.4±0.1	921 ± 140
<b><math>35 &lt; M_{vis} &lt; 80 \text{ GeV}</math></b>	<b>5±1</b>	4±1 [1]	8±2 [1]	2±1 [0.67]	<1.6	0.3±0.1 [1]	745 ± 112 [0.80]

Muon+TauJet Opposite Sign



Muon+TauJet Same Sign

